

RESEARCH PAPER



In vitro and *in silico* studies of bis (indol-3-yl) methane derivatives as potential α -glucosidase and α -amylase inhibitors

Peng-Fei Zheng^a, Zhuang Xiong^b, Cui-ying Liao^b, Xin Zhang^b, Mei Feng^b, Xiao-Zheng Wu^b, Jing Lin^b, Lin-Sheng Lei^c, You-Cheng Zhang^a, Shao-Hua Wang^c and Xue-Tao Xu^b

^aSecond Hospital of Lanzhou University, Lanzhou, PR China; ^bSchool of Biotechnology and Health Sciences, Wuyi University, Jiangmen, PR China; ^cSchool of Pharmacy & State Key Laboratory of Applied Organic Chemistry, Lanzhou University, Lanzhou, PR China

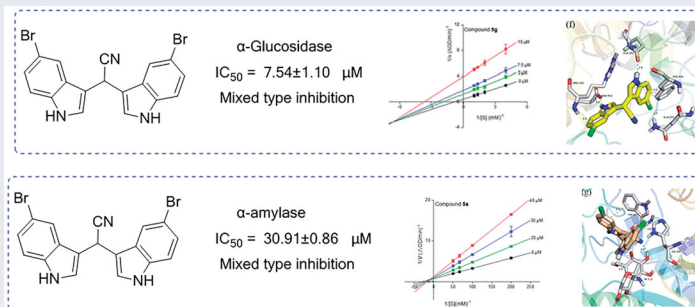
ABSTRACT

In this paper, bis (indol-3-yl) methanes (BIMs) were synthesised and evaluated for their inhibitory activity against α -glucosidase and α -amylase. All synthesised compounds showed potential α -glucosidase and α -amylase inhibitory activities. Compounds **5g** (IC_{50} : $7.54 \pm 1.10 \mu M$), **5e** (IC_{50} : $9.00 \pm 0.97 \mu M$), and **5h** (IC_{50} : $9.57 \pm 0.62 \mu M$) presented strongest inhibitory activities against α -glucosidase, that were ~ 30 times stronger than acarbose. Compounds **5g** (IC_{50} : $32.18 \pm 1.66 \mu M$), **5h** (IC_{50} : $31.47 \pm 1.42 \mu M$), and **5s** (IC_{50} : $30.91 \pm 0.86 \mu M$) showed strongest inhibitory activities towards α -amylase, ~ 2.5 times stronger than acarbose. The mechanisms and docking simulation of the compounds were also studied. Compounds **5g** and **5h** exhibited bifunctional inhibitory activity against these two enzymes. Furthermore, compounds showed no toxicity against 3T3-L1 cells and HepG2 cells.

HIGHLIGHTS

1. A series of bis (indol-3-yl) methanes (BIMs) were synthesised and evaluated inhibitory activities against α -glucosidase and α -amylase.
2. Compound **5g** exhibited promising activity ($IC_{50} = 7.54 \pm 1.10 \mu M$) against α -glucosidase.
3. Compound **5s** exhibited promising activity ($IC_{50} = 30.91 \pm 0.86 \mu M$) against α -amylase.
4. *In silico* studies were performed to confirm the binding interactions of synthetic compounds with the enzyme active site.

GRAPHICAL ABSTRACT



ARTICLE HISTORY

Received 22 June 2021
Revised 10 August 2021
Accepted 15 August 2021

KEYWORDS

Bis (indol-3-yl) methanes;
 α -Glucosidase; α -Amylase;
inhibitor; molecular docking

1. Introduction

Diabetes mellitus (DM) is one of common metabolic disease characterised by hyperglycaemia.¹ The main clinical treatment strategies for DM is to control the blood glucose level using drugs.² The catalytic hydrolysis of carbohydrates by enzymes such as α -glucosidase and α -amylase is the most important reason for the increase of glucose in blood.³

α -Glucosidase (EC 3.2.1.20), existing in the surface of small intestine, is an important hydrolase enzyme.^{4–5} It catalyses the hydrolysis of carbohydrates into absorbable glucose monomers by splitting the bond between glucosidic oxygen and glucosyl

residues of carbohydrates.^{6–7} α -Amylase (E.C.3.2.1.1), one hydrolase enzyme, is mainly secreted by the pancreas and salivary glands.^{8–9} α -Amylase catalytic hydrolyse the starch to produces maltose and glucose by breaking α -1,4-glucosidic bonds.^{10–11} The inhibition the activity of α -glucosidase or α -amylase delay the hydrolase of polysaccharides, consequently, the postprandial blood glucose level can be reduced, which is believed as an effective approach for the treatment strategy of DM. To date, a large amount of α -glucosidase and α -amylase inhibitors are obtained from natural products and chemical synthesis.^{12–15} However only few have further application, such as acarbose, voglibose, and miglitol. However, these

CONTACT You-Cheng Zhang  zhangychmd@126.com; Shao-Hua Wang  wangshh@lzu.edu.cn; Xue-Tao Xu  wuychemxxt@126.com

© 2021 The Author(s). Published by Informa UK Limited, trading as Taylor & Francis Group.

This is an Open Access article distributed under the terms of the Creative Commons Attribution License (<http://creativecommons.org/licenses/by/4.0/>), which permits unrestricted use, distribution, and reproduction in any medium, provided the original work is properly cited.

clinical drugs are often associated with side-effects. Therefore, it is still worth further investigation for the development of more effective inhibitors towards α -glucosidase and α -amylase.

Bis (indol-3-yl) methanes (BIMs), as the key skeletons, present in a variety of bioactive natural products isolated from marine organisms, land plants and microorganisms.^{16–18} And such a fact has also stimulated the synthesis of different BIMs leading to the reveal of a wide range of bio-pharmacological activities, including anti-fungal, anti-inflammatory, anti-oxidant, anti-cancer, and anti-bacterial activities.^{19–22} Especially, it is notable that BIMs are reported to process activities of lowering blood lipids and preventing obesity²³ as well as inhibiting α -glucosidase activity, showing great potential in the treatment of DM. In order to find potential α -glucosidase inhibitors, some BIMs were synthesised and presented effective inhibitory activity.^{24–25}

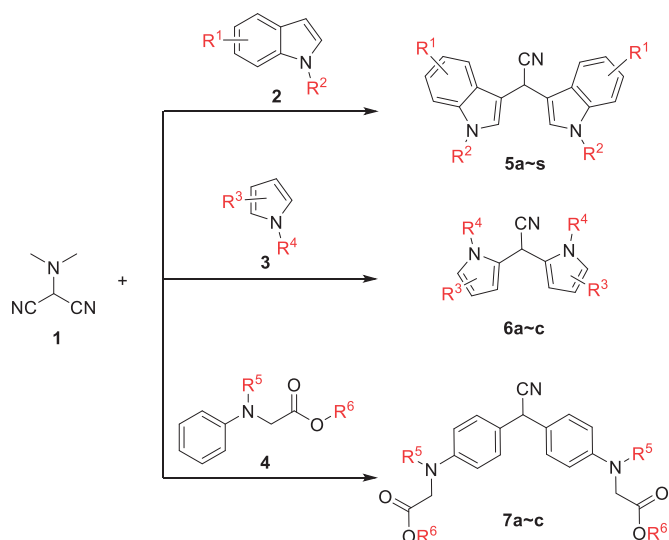
The cyano group, a carbon-nitrogen triple bond, has been widely used in the structural modification and transformation of small drug molecules. It can change the physical and chemical properties of small molecules, enhance the interaction between drug molecules and target proteins to improve drug efficacy, improve the metabolic stability of compounds in the body, and so on.²⁶ The cyano group also is used as an important substitution group in some reported α -glucosidase inhibitors.^{27–28}

Based on the principle of combination of active structural moieties in drug design and our synthetic methodology for BIMs derivatives,²⁹ we synthesised BIMs derivatives to evaluate them for their α -glucosidase and α -amylase inhibitory activity.

2. Results and discussion

2.1. Chemistry

Based on the effective synthetic method of BIMs reported by our group, **5a–c**, **6a–c**, and **7a–c** were synthesised from *N,N*-dimethylaminomalononitrile (**1**) with substituted indole (**2**), substituted pyrrole (**3**) or *N*-phenylaminoacetic acid ethyl ether (**4**) under the catalysis of $\text{Al}(\text{OTf})_3$. The synthetic route was shown in Scheme 1. All synthetic compounds are known compounds, which were reported in references.²⁹



Scheme 1 Synthesis of BIMs. Reagents and conditions: $\text{Al}(\text{OTf})_3$ (0.2 equiv.), DCE, 120°C, 8 h.

2.2. Evaluation of activity against α -glucosidase

2.2.1. α -Glucosidase inhibition assay

The *in vitro* α -glucosidase inhibitory activities of all synthesised compounds were evaluated using *p*-nitrophenyl- α -D-glucopyranoside (PNPG) as substrate. As shown in Table 1, BIMs **5a–c** (IC_{50} : 7.54 ± 1.10 to $150.48 \pm 3.16 \mu\text{M}$) presented good inhibitory activities, stronger than acarbose (IC_{50} : $261.45 \pm 2.17 \mu\text{M}$). Among them, **5g**, **5e**, and **5h** displayed strongest inhibitory activities with the IC_{50} values of 7.54 ± 1.10 , 9.00 ± 0.97 and $9.57 \pm 0.62 \mu\text{M}$, respectively, those were ~ 30 times stronger than that of acarbose. While, **6a–c**, **7a–c** showed moderate inhibitory activities with IC_{50} values from 100.38 ± 0.53 to $242.78 \pm 5.14 \mu\text{M}$.

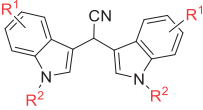
2.2.2. Structure activity relationships (SAR) analysis

The SAR of compounds was discussed by analysing the substitution pattern on indole moiety. Compound **5a** (IC_{50} = $55.53 \pm 0.40 \mu\text{M}$) with no substitution on indole ring showed ~ 5 fold stronger compared to acarbose (IC_{50} = $261.45 \pm 2.17 \mu\text{M}$). Compound **5r** (IC_{50} = $100.96 \pm 1.69 \mu\text{M}$) with a methyl group at 1-position of indole presented decreased activity. However, introducing bromine group on the indole ring of **5r**, compound **5s** (IC_{50} = $30.48 \pm 1.27 \mu\text{M}$), caused obviously increase in inhibition activity. The introduction of two phenyl groups at the 2-position of indole ring (compound **5h**, IC_{50} = $9.57 \pm 0.62 \mu\text{M}$) resulted in markedly increase of activity (Figure 1). The above results indicated possible hydrogen bond interaction between compound **5a** and α -glucosidase, halogen bond between **5s** and glucosidase, as well strong π - π stacking effect between **5h** and α -glucosidase.

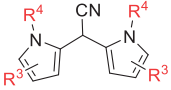
Compared to compound **5a**, compounds **5c–5f** with chlorine substituent on the benzene ring of indole had more potent activities. This indicated that chlorine atom, a typical halogen atom, might be well interact with α -glucosidase through halogen bond like that of compound **5s** (Figure 2). Among chlorine substituted derivatives, **5e** (IC_{50} = $9.00 \pm 0.97 \mu\text{M}$) with the 6-chlorine group was found to be most active and 29 times better activity than acarbose. It's positional isomer **5d** (IC_{50} = $10.22 \pm 0.63 \mu\text{M}$) with 5-chlorine group, presented similar activity. However, **5c** (IC_{50} = $45.10 \pm 1.42 \mu\text{M}$) and **5f** (IC_{50} = $20.65 \pm 0.42 \mu\text{M}$) with 4-chlorine group and 7-chlorine group respectively showed lower activities.

Compounds **5i–o** with methyl group on the indole ring showed moderate inhibitory activities. This indicated that methyl group, an electron donating group, had no beneficial effects on the interaction with α -glucosidase (Figure 3). Compared to compound **5a**, introduction of 6-methyl group **5l** (IC_{50} = $50.64 \pm 1.78 \mu\text{M}$) and 5-methyl group **5k** (IC_{50} = $50.64 \pm 1.78 \mu\text{M}$) resulted in slight changes on inhibitory activities, while presence of 2-methyl group **5i** (IC_{50} = $120.83 \pm 4.45 \mu\text{M}$), 4-methyl group **5j** (IC_{50} = $70.53 \pm 1.42 \mu\text{M}$), 7-methyl group **5m** (IC_{50} = $150.48 \pm 3.16 \mu\text{M}$), and 2,5-dimethyl groups **5o** (IC_{50} = $65.06 \pm 0.61 \mu\text{M}$) caused obvious decrease on the activity. When introducing 5-fluorine group, compound **5n** (IC_{50} = $50.97 \pm 0.69 \mu\text{M}$) and 5-methyl group, compound **5o** (IC_{50} = $65.06 \pm 0.61 \mu\text{M}$) showed visible increase on the inhibitory activity, as compared to compound **5i**. This might be attributed to possible hydrogen bond interaction formed by fluorine atom.

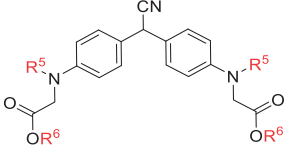
Analysing effect of different type of substituent at same substituent position (Figure 4), halogen atom substituents lead to strengthen of α -glucosidase inhibitory activities, while electron donating and withdrawing groups resulted in decrease of the activity, as compared to compound **5a**. Compound **5g** (IC_{50} = $7.54 \pm 1.10 \mu\text{M}$) with 5-bromine groups presented 34 times stronger activity than acarbose, and **5b** (IC_{50} = $40.86 \pm 0.27 \mu\text{M}$) with 5-

Table 1. α -Glucosidase and α -amylase inhibitory activity of all synthesised compounds.


Compounds	R ¹	R ²	IC ₅₀ (μ M) on α -glucosidase	IC ₅₀ (μ M) on α -amylase
5a	H	H	55.53 \pm 0.40	493.59 \pm 10.34
5b	5-F	H	40.86 \pm 0.27	147.09 \pm 6.23
5c	4-Cl	H	45.10 \pm 1.42	151.25 \pm 5.21
5d	5-Cl	H	10.22 \pm 0.63	41.95 \pm 1.97
5e	6-Cl	H	9.00 \pm 0.97	40.03 \pm 2.14
5f	7-Cl	H	20.65 \pm 0.42	266.86 \pm 3.87
5g	5-Br	H	7.54 \pm 1.10	32.18 \pm 1.66
5h	2-Ph	H	9.57 \pm 0.62	31.47 \pm 1.42
5i	2-CH ₃	H	120.83 \pm 4.45	123.44 \pm 3.27
5j	4-CH ₃	H	70.53 \pm 1.42	151.60 \pm 2.94
5k	5-CH ₃	H	55.99 \pm 0.78	406.31 \pm 8.44
5l	6-CH ₃	H	50.64 \pm 1.78	36.35 \pm 1.37
5m	7-CH ₃	H	150.48 \pm 3.16	500.41 \pm 13.57
5n	5-F,2-CH ₃	H	50.97 \pm 0.69	154.05 \pm 3.08
5o	5-CH ₃ ,2-CH ₃	H	65.06 \pm 0.61	472.77 \pm 7.65
5p	5-OCH ₃	H	50.37 \pm 1.06	137.81 \pm 5.62
5q	5-COOCH ₃	H	80.12 \pm 0.79	205.36 \pm 4.87
5r	H	CH ₃	100.96 \pm 1.69	153.04 \pm 3.43
5s	5-Br	CH ₃	30.48 \pm 1.27	30.91 \pm 0.86



Compounds	R ³	R ⁴	IC ₅₀ (μ M)	IC ₅₀ (μ M)
6a	H	CH ₃	220.31 \pm 5.02	463.96 \pm 9.47
6b	2-CH ₃	H	120.77 \pm 3.51	435.62 \pm 10.65
6c	H	H	130.36 \pm 3.81	418.71 \pm 11.32



Compounds	R ⁵	R ⁶	IC ₅₀ (μ M)	IC ₅₀ (μ M)
7a	CH ₃	CH ₂ CH ₃	100.38 \pm 0.53	510.16 \pm 12.55
7b	H	CH ₂ CH ₃	180.05 \pm 0.79	139.21 \pm 4.85
7c	H	CH ₃	242.78 \pm 5.14	479.17 \pm 13.44
Acarbose			261.45 \pm 2.17	80.33 \pm 2.95

fluorine groups displayed 6 times stronger activity than acarbose. However, compound **5k** ($IC_{50} = 55.99 \pm 0.78 \mu\text{M}$) with 5-methyl group and **5p** ($IC_{50} = 50.37 \pm 1.06 \mu\text{M}$) with 5-methoxy group exhibited lower activities than that of **5a**. In addition, the introduction of electron withdrawing group, methyl formate, **5q** ($IC_{50} = 80.12 \pm 0.79 \mu\text{M}$) resulted in a decrease on the α -glucosidase inhibitory activity.

Compared to series of **5a~s**, **6a~c** and **7a~c** only presented moderate α -glucosidase inhibitory activities with IC_{50} values from $100.38 \pm 0.53 \mu\text{M}$ to $242.78 \pm 5.14 \mu\text{M}$, indicating that indole ring might be more beneficial than pyrrole ring and benzene ring on α -glucosidase inhibitory activities.

2.2.3. Inhibition mechanism study of α -glucosidase inhibitor

To gain further insight into the interaction between BIMs and α -glucosidase, the inhibition mechanism of compounds **5e**, **5g**, and **5h** with highly potent inhibitory were investigated. The relationship of enzyme concentration with enzyme activity in presence of compounds **5e**, **5g**, and **5h** was firstly investigated. As shown in Figure 5, the plots of enzyme concentration vs

remaining enzyme activity at different inhibitor concentrations give a group of straight lines that all passed through the origin point. Those results indicated that the α -glucosidase inhibition of compounds **5e**, **5g**, and **5h** was reversible.

The inhibitory kinetics of compounds **5e**, **5g**, and **5h** on α -glucosidase were studied using Lineweaver-Burk plots. For compounds **5e**, **5g**, and **5h**, the plots of $1/v$ vs $1/[S]$ give a lot of straight lines that intersected at the same point in the third quadrant respectively (Figure 6), revealing that compounds **5e**, **5g**, and **5h** were all mixed-type inhibitors. These results indicated that compounds **5e**, **5g**, and **5h** could bind with free enzyme, as well as, enzyme-substrate complex to reduce the catalytic activity of α -glucosidase.

Besides, we also determined the equilibrium constants of binding of inhibitors to free enzymes (K_i) and enzyme-substrate complexes (K_{iS}) through plots of slope (K_m/V_m) and vertical intercept ($1/V_m$) vs inhibitor concentration. The results were presented in Table 2. The K_i values of compounds **5e**, **5g**, and **5h** were higher than their K_{iS} values, suggesting that the affinity of compounds **5e**, **5g**, and **5h** with free enzyme was lower than that with enzyme-substrate complex.

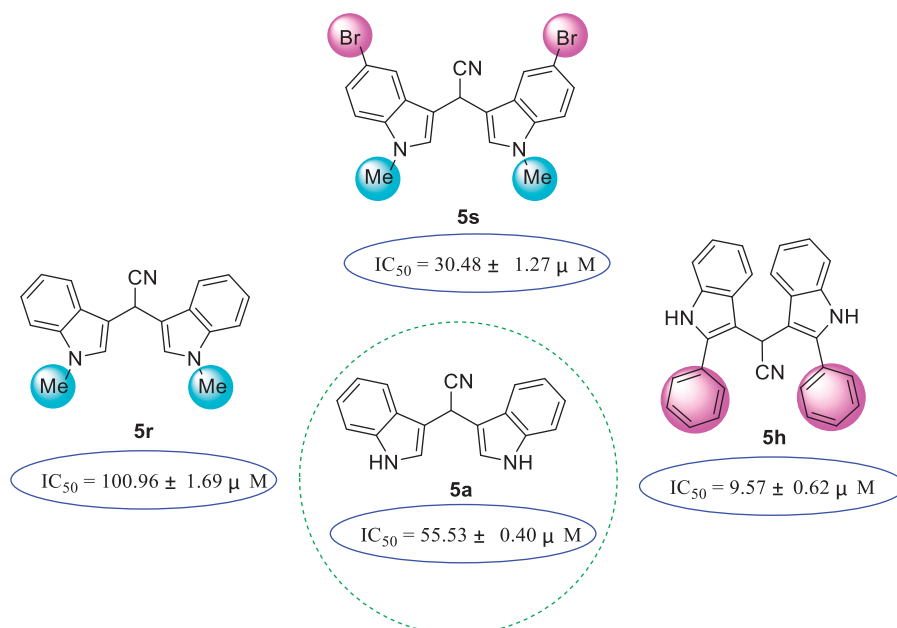


Figure 1. SAR analysis of compounds **5a**, **5r**, and **5s**.

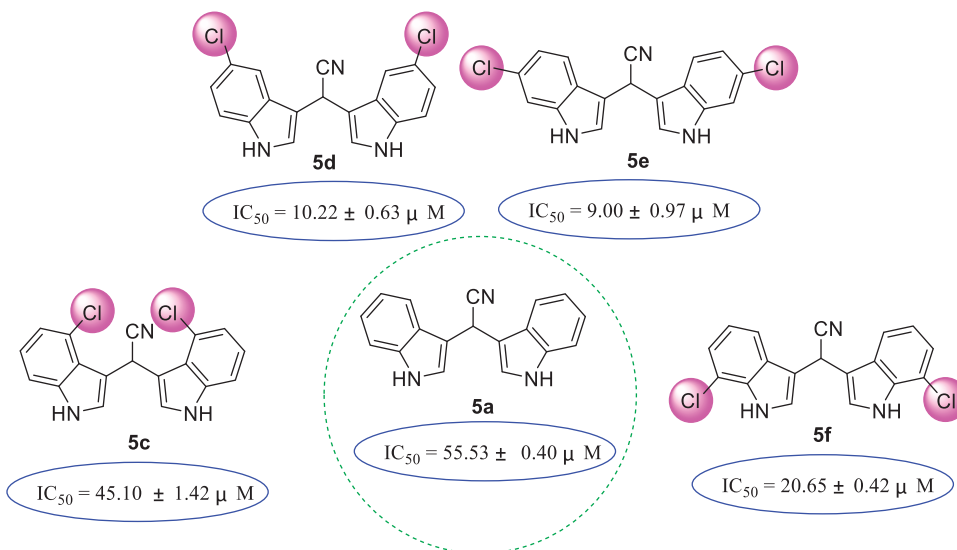


Figure 2. SAR analysis of compounds **5a**, **5c**–**5f**.

2.2.4. Molecular docking study

Sybyl molecular docking program was used to simulate the binding modes of α -glucosidase with the topmost active compounds, i.e. **5e**, **5g**, and **5h** to further understand the inhibition mechanism. As shown in Figure 7(a–d), compound **5e** (orange compound), **5h** (yellow compound), and **5g** (cyan compound), were well nested into the active site of α -glucosidase and presented similar coordination with the active site of enzyme. The docking of compound **5e** was presented in Figure 7(e). One indole ring nitrogen formed a hydrogen bond (2.0 Å) with Asp307, another indole ring nitrogen formed a hydrogen bond (1.9 Å) with Glu277, and cyano nitrogen formed a hydrogen bond (2.6 Å) with Arg315. Also, chlorine on indole ring formed a halogen bond with Arg442 (3.3 Å). For compound **5g** (Figure 7(f)), The two indole ring nitrogen made two hydrogen bonds with Gln353 (1.9 Å) and Glu411 (2.0 Å), respectively, and the two chlorines on indole ring made two halogen bond with Arg315 (2.0 Å) and Gln279 (3.7 Å), respectively. Moreover, one indole ring made π - π interactions with

Phe303 (3.9 Å). Compounds **5h** (Figure 7(g)) also formed a hydrogen bond with Asp307 (2.0 Å), and formed π - π interactions with Phe303 (4.3 Å) and Tyr158 (4.5 Å), respectively. The hydrogen bond, π - π interactions, or halogen bond existed between α -glucosidase with compounds **5e**, **5g**, or **5h** played very important roles in the binding of compounds and proteins.

2.3. Evaluation of activity against α -amylase

2.3.1. α -Amylase inhibition assay

Meantime, all compounds were tested for α -amylase inhibitory activity *in vitro* and their IC_{50} values were recorded in Table 1. All synthesised BIMs displayed good to moderate inhibitory activities, IC_{50} range of $30.91 \pm 0.86 \sim 510.16 \pm 12.55 \mu M$. Excitingly, compounds **5g** (IC_{50} : $32.18 \pm 1.66 \mu M$), **5h** (IC_{50} : $31.47 \pm 1.42 \mu M$), and **5s** (IC_{50} : $30.91 \pm 0.86 \mu M$) showed strongest inhibitory activities, ~ 2.5 times stronger than that of acarbose (IC_{50} : $80.33 \pm 2.95 \mu M$).

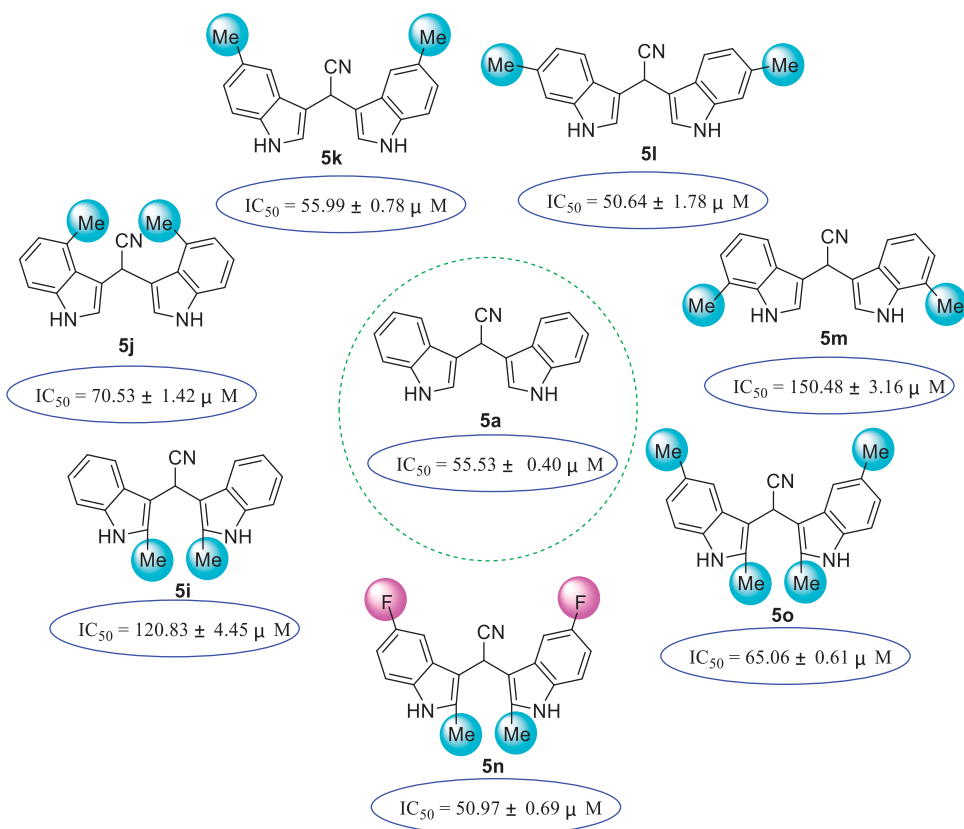


Figure 3. SAR analysis of compounds 5a, and 5i~o.

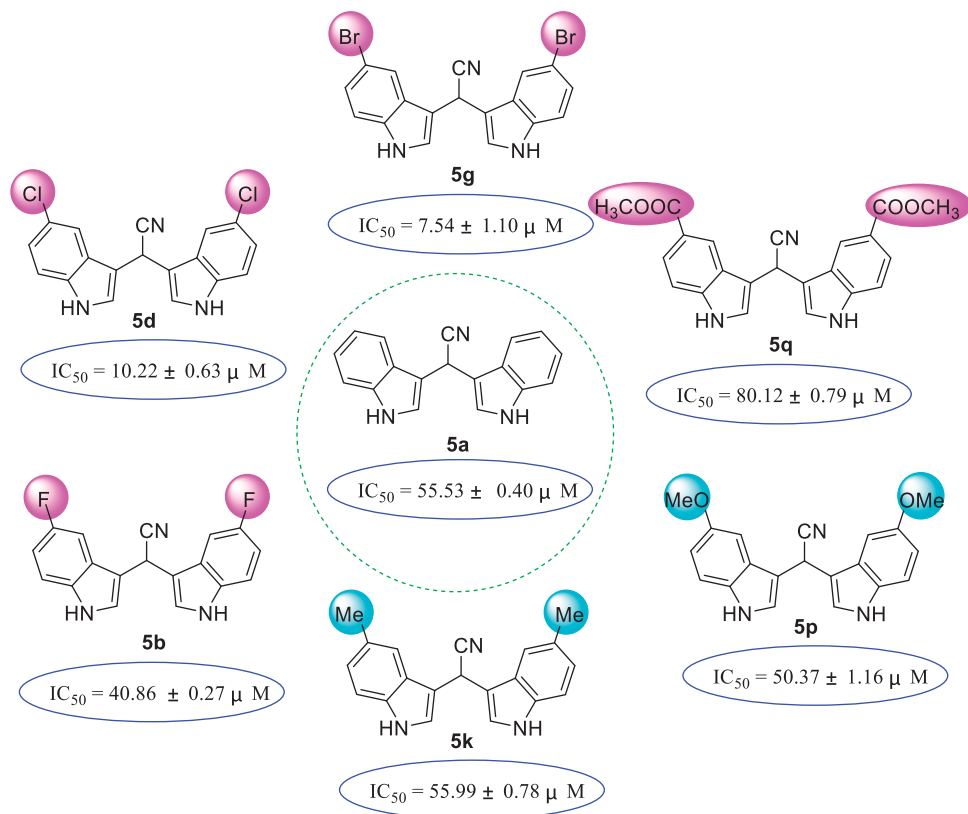


Figure 4. SAR analysis of compounds 5a, 5b, 5d, 5g, 5q, 5p, and 5k.

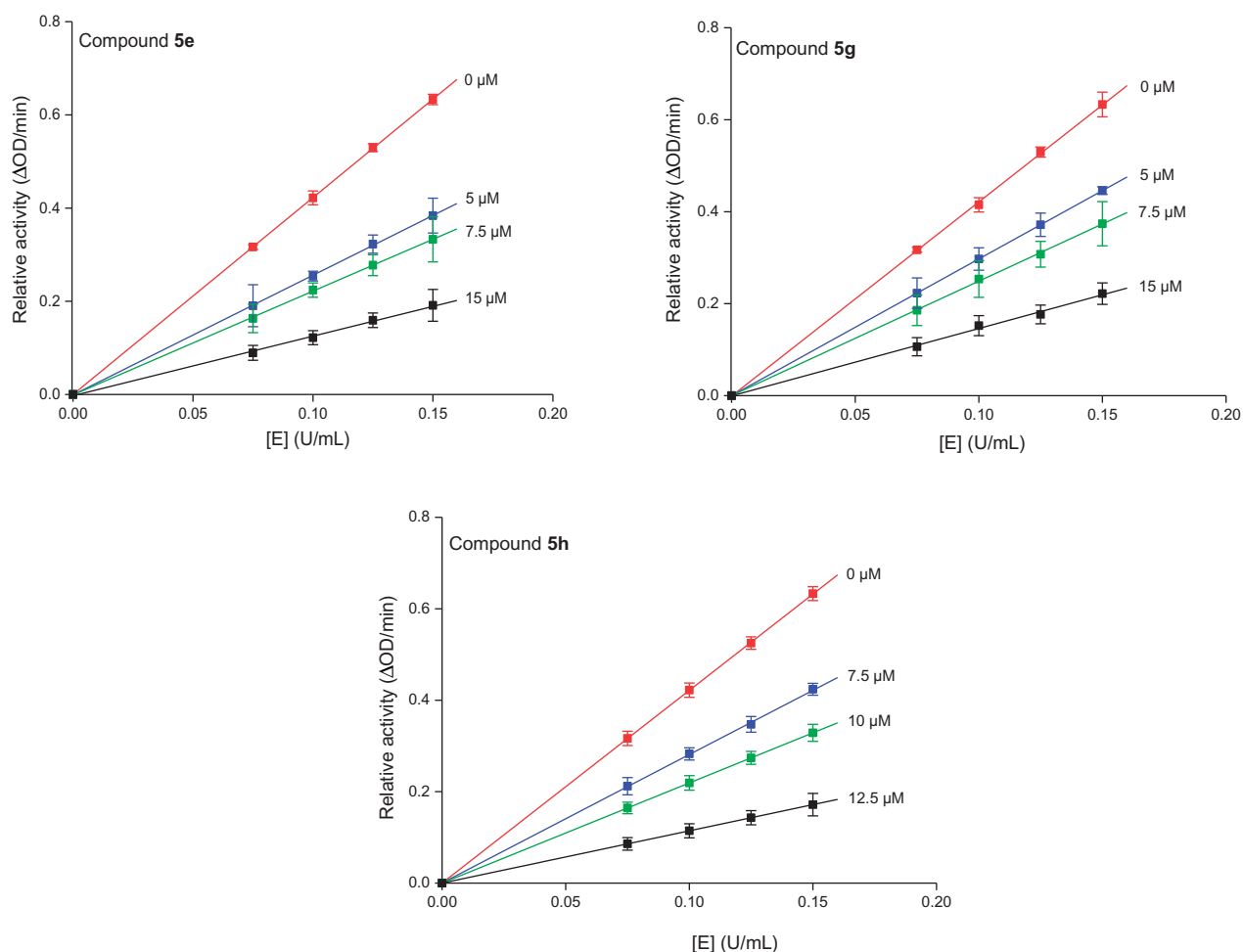


Figure 5. The plots of α -glucosidase concentration vs enzyme activity in presence of compounds **5e**, **5g**, and **5h**.

2.3.2. Sar analysis

The SAR of all compounds against α -amylase were also analysed with compound **5a** (IC_{50} : $493.59 \pm 10.34 \mu M$) as template compound. The introduction of halogen (F, Cl, Br) on indole ring effectively increased the inhibitory activity, Br group (compound **5g**, IC_{50} : $32.18 \pm 1.66 \mu M$) is most beneficial for the inhibitory activity, and Cl group at 6-position (compound **5e**, IC_{50} : $40.03 \pm 2.14 \mu M$) of indole presented better inhibitory activity compared to other position. The introduction of methyl group also changed the inhibitory activity, and compound **5i** with methyl group at 6-position (IC_{50} : $36.35 \pm 1.37 \mu M$) presented the best inhibitory activity. The introduction of methoxy, Phenyl, and ester group also increased the inhibitory activity, especially, compound **5h** with Phenyl group (IC_{50} : $31.47 \pm 1.42 \mu M$) extended good inhibitory activity. Furthermore, compounds **6a~c** and **7a~c** presented effectively lower α -amylase inhibitory activities than compounds **5a~s**, indicating that indole ring was more helpful for α -amylase inhibitory activities.

2.3.3. Inhibition mechanism study of α -amylase inhibitor

The highest potent inhibitory compounds **5g**, **5h**, and **5s** were evaluated their inhibition mechanism. As shown in Figure 8, the remaining enzyme activity at different inhibitor concentrations was measured and the obtained straight lines passed through the origin point, suggesting that compounds **5g**, **5h**, and **5s** reversibly inhibited the α -amylase. Lineweaver-Burk plots were used to

analyse the inhibitory kinetics of compounds **5g**, **5h**, and **5s**. The plots of $1/v$ vs $1/[S]$ intersected a point at the second quadrant, indicating that **5g**, **5h**, and **5s** were mixed inhibitors (Figure 9). Besides, the K_i and K_{is} values of compounds **5g**, **5h**, and **5s** were measured, showing K_i values were higher than K_{is} values (Table 3).

2.3.4. Docking simulation for α -amylase

As mentioned above, molecular docking between compounds **5g**, **5h**, and **5s** with α -amylase were used to explain their mechanism. Docking results revealed that compounds **5g** (yellow compound), **5h** (cyan compound), and **5s** (wheat compound) were well located within the active site of α -amylase (Figure 10(a-d)). Binding models of compounds **5g**, **5h**, and **5s** with α -amylase were depicted in Figure 10(e-f), respectively. For compound **5g**, cyano nitrogen made a hydrogen bond with His305 (2.8 Å), and chlorine on indole ring made a halogen bond with Trp59 (3.1 Å) and one indole ring made π - π interactions with Trp59 (3.1 Å). The docking of compound **5e** showed that one indole ring nitrogen formed a hydrogen bond (2.2 Å) with Ac1_2, and two indole rings formed π - π interactions with Trp59 (4.4 and 5.3 Å). The indole ring nitrogen and cyano nitrogen of compounds **5s** also formed two hydrogen bonds with Ac1_2 (2.5 and 2.5 Å), a hydrogen bond with His305 (3.9 Å), and π - π interactions with Trp59 (5.5 Å), respectively. The hydrogen bond, π - π interactions, or halogen bond existed between α -amylase with compounds **5g**, **5h**, or **5s**

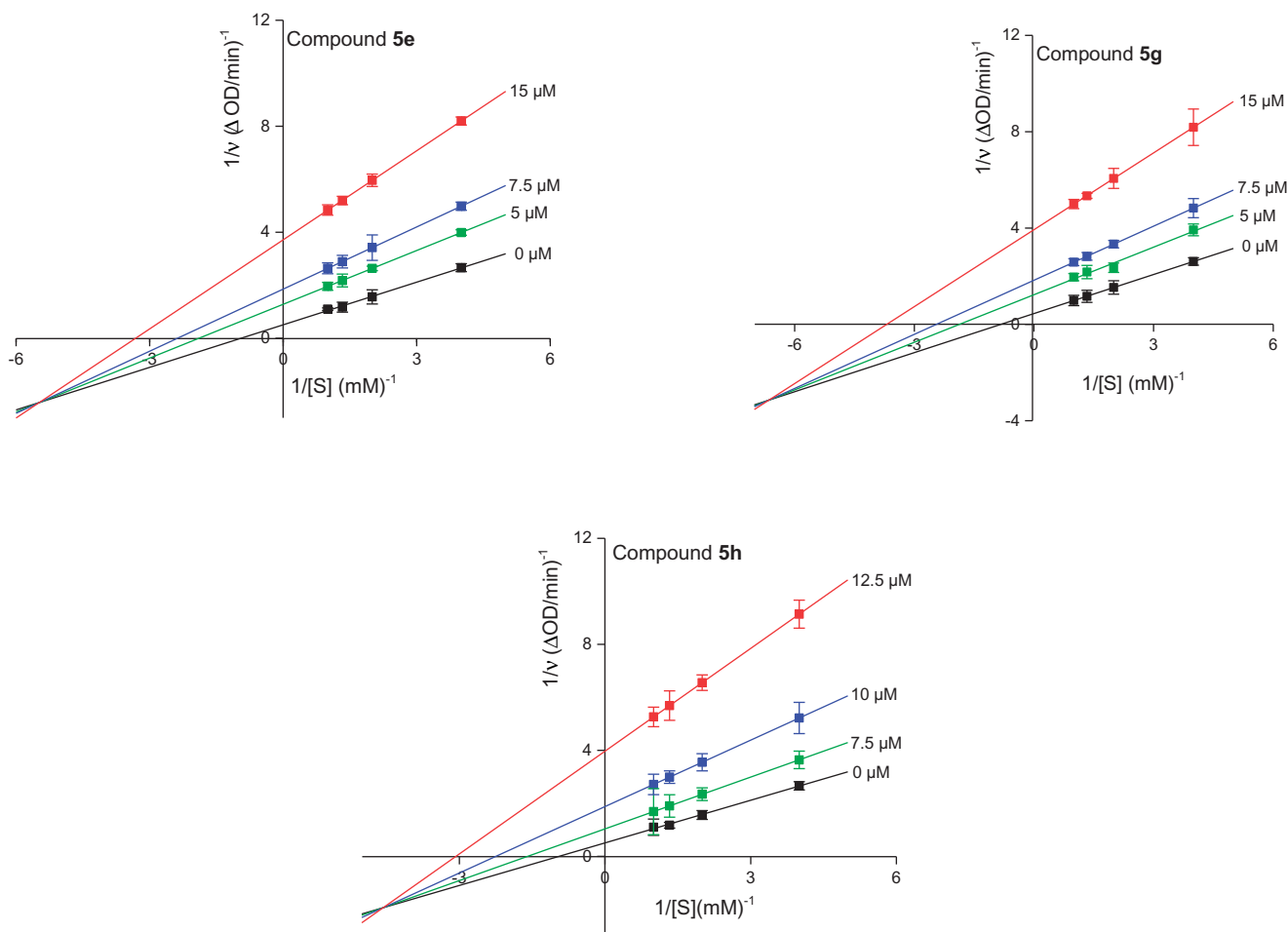


Figure 6. Lineweaver-Burk plots of α -glucosidase inhibition by compounds **5e**, **5g**, and **5h**.

Table 2. The inhibition type, as well as K_i and K_{iS} values of **5e**, **5g**, and **5h** against α -glucosidase.

Compound	Inhibition type	K_i value (μM)	K_{iS} value (μM)
5e	Mixed type	13.36	2.11
5g	Mixed type	14.93	1.59
5h	Mixed type	8.71	1.69

were helpful to stabilise the formation of the ligand-protein complex.

Based on above assays results of compounds targeting α -glucosidase and α -amylase, compounds **5e**, **5g**, and **5h** showed highest α -glucosidase inhibitory and compounds **5g**, **5h**, and **5s** presented highest α -amylase inhibitory. Thence, compounds **5g** and **5h** displaying the potential bifunctional could be considered as the lead compounds for bifunctional drugs.

2.4. *In vitro* cytotoxicity assay

Moreover, the preliminary *in vitro* safety of compounds **5e**, **5g**, **5h**, and **5s** were tested on Mouse Preadipocytes cells (3T3-L1) and Human liver cancer cells (HepG2) using MTT method and the results were shown in Figure 11. Compounds **5e**, **5g**, **5h**, and **5s** displayed no effect on the viability of 3T3-L1 cells and HepG2 cells at concentration range of 2.0 ~ 80 μM , suggesting these promising inhibitors had non-toxic towards live cells.

3. Conclusion

For searching α -glucosidase and α -amylase inhibitor, a variety of synthetic BIMs were prepared and assayed. Compounds **5g** (IC_{50} : $7.54 \pm 1.10 \mu\text{M}$), **5e** (IC_{50} : $9.00 \pm 0.97 \mu\text{M}$), and **5h** (IC_{50} : $9.57 \pm 0.62 \mu\text{M}$) were the strongest inhibitor against α -glucosidase and compounds **5g** (IC_{50} : $32.18 \pm 1.66 \mu\text{M}$), **5h** (IC_{50} : $31.47 \pm 1.42 \mu\text{M}$), and **5s** (IC_{50} : $30.91 \pm 0.86 \mu\text{M}$) were the strongest inhibitor against α -amylase. The mechanisms results revealed that compounds were reversible mixed-type inhibitors. Molecular docking explained the action mechanism between inhibitors and target proteins. Finally, their low toxicity to 3T3-L1 cells and HepG2 cells lays the foundation for *in vivo* studies.

4. Materials and methods

4.1. Chemistry

α -Glucosidase, α -amylase, 4-Nitrophenyl- β -D-galactopyranoside (PNPG) and 3-(4,5-Dimethylthiazol-2-yl)-2,5-diphenyl-tetrazolium-bromide (MTT) were supplied by Sigma-Aldrich. Water-soluble starch was obtained from Shanghai Yuanye Biological Technology Co.,Ltd. 3T3-L1 cells and HepG2 cells were supplied by ATCC. Dulbecco's Modified Eagle's Medium (DMEM), Foetal bovine serum (FBS), penicillin and streptomycin were obtained from Gibco. All commercially available compounds were used without further purification. All reactions under standard conditions were carried out under argon and dry atmosphere.¹H and ¹³C spectra were

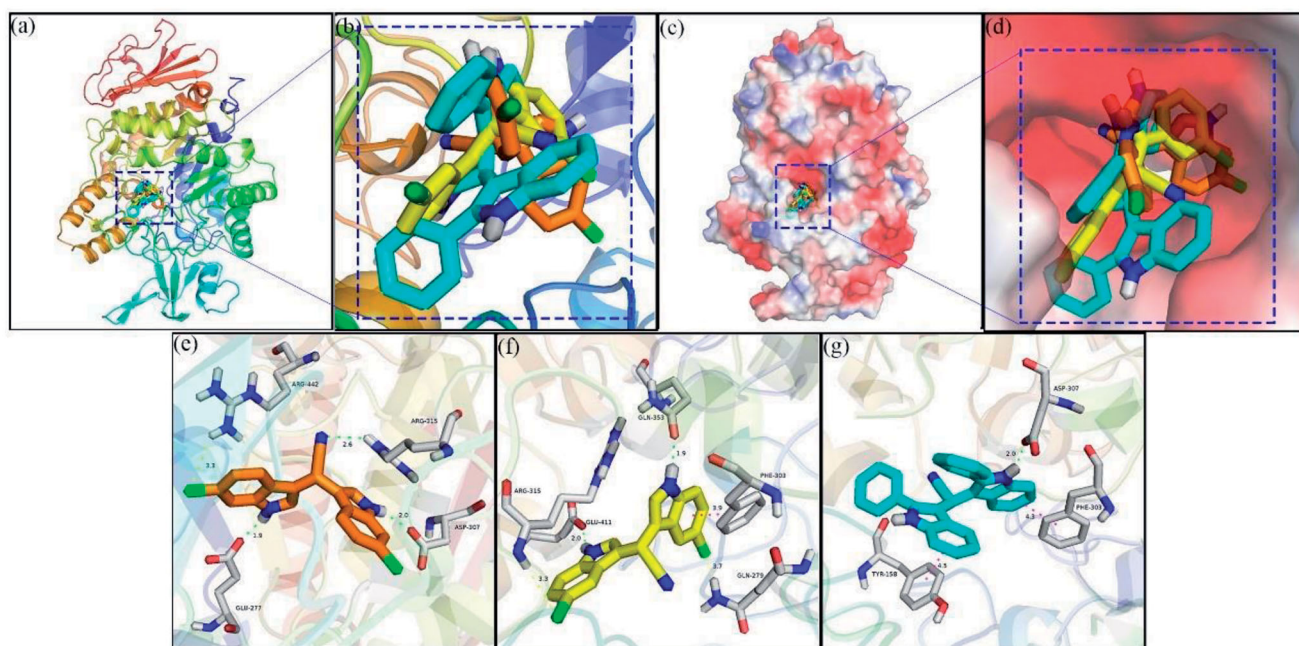


Figure 7. Molecular docking of compounds 5e, 5g, and 5h with α -glucosidase.

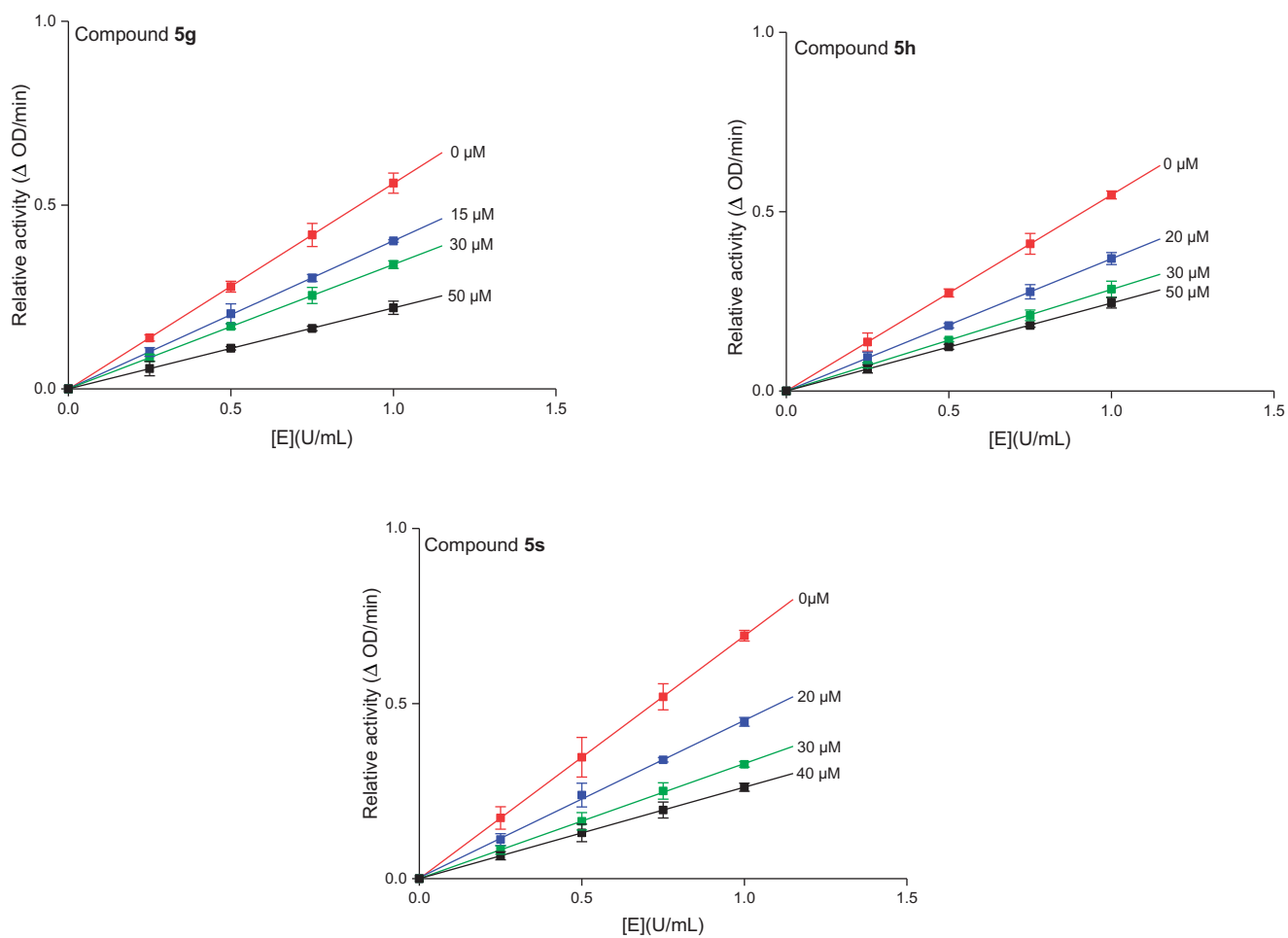


Figure 8. The relationship of α -amylase concentration with α -amylase activity in presence of compounds 5g, 5h, and 5s.

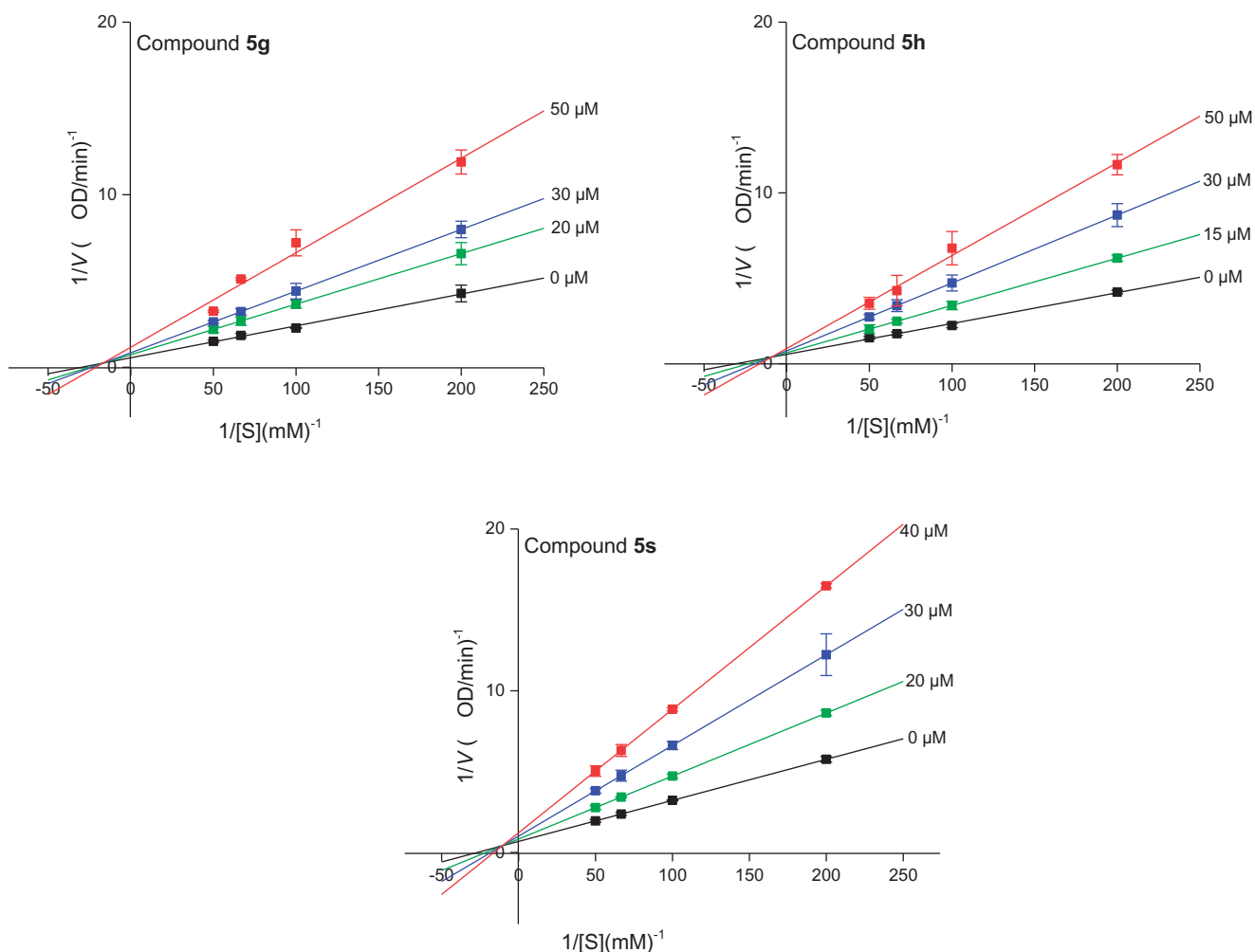


Figure 9. Lineweaver-Burk plots of α -amylase inhibition by compounds **5e**, **5g**, and **5h**.

Table 3. The inhibition type, as well as K_i and K_{IS} values of **5g**, **5h**, and **5s** against α -amylase.

Compound	Inhibition type	K_i value (μM)	K_{IS} value (μM)
5g	Mixed type	78.33	25.02
5h	Mixed type	37.39	1.63
5s	Mixed type	25.98	9.01

recorded in CDCl_3 , $\text{DMSO-}d_6$, $\text{Acetone-}d_6$ on 400 MHz instruments and spectral data were reported in ppm. High-resolution mass spectral analysis (HRMS) data were measured on the Apex II by means of the ESI technique.

4.2. ENERAL procedure for the preparation of derivatives (**5a** ~ **c**, **6a** ~ **c**, **7a** ~ **c**)

N,N-dimethylaminomalononitrile (**1**) (1.2 mmol), substituted indole (**2**) (1 mmol), and $\text{Al}(\text{OTf})_3$ (0.20 mmol) were added into DCE (2 ml), then the mixture was stirred at 120°C under argon atmosphere until the reaction was complete (monitored by TLC). The mixture was evaporated to give the crude product, followed purification to produce **5a**~**c**. Likewise, compounds **6a**~**c** were obtained from *N,N*-dimethylaminomalononitrile (**1**) and substituted pyrrole (**3**), compounds **7a**~**c** were synthesised from *N,N*-dimethylaminomalononitrile (**1**) and *N*-phenylaminoacetic acid ethyl ether.

4.2.1. 2,2-Di(1*H*-indol-3-yl)acetonitrile (**5a**)

Rf = 0.35 (petroleum ether/ethyl acetate = 2: 1); White solid; Yield 89%; m.p.: 173.9 – 178.3°C ; ^1H NMR (600 MHz, $\text{DMSO-}d_6$) δ 11.17 (s, 2H), 7.59 (d, $J = 7.8$ Hz, 2H), 7.43–7.41 (m, 4H), 7.12 (t, $J = 7.8$ Hz, 2H), 7.00 (t, $J = 7.8$ Hz, 2H), 6.08 (s, 1H); ^{13}C NMR (150 MHz, $\text{DMSO-}d_6$) δ 136.54, 125.20, 123.69, 121.52, 120.68, 118.87, 118.49, 111.84, 109.43, 25.29; HRMS (ESI) calcd for $\text{C}_{18}\text{H}_{13}\text{N}_3$ [$\text{M} + \text{Na}$] $^+$: 294.1002, found 294.1013; IR ν (cm^{-1}): 3411, 3057, 2924, 2854, 2242, 1620, 1457, 1338, 1097, 743.

4.2.2. 2,2-Bis(5-fluoro-1*H*-indol-3-yl)acetonitrile (**5b**)

Rf = 0.41 (petroleum ether/ethyl acetate = 1: 1); Yellow solid; Yield 89%; m.p.: 182.7 – 187.5°C ; ^1H NMR (400 MHz, $\text{Acetone-}d_6$) δ 10.51 (s, 2H), 7.57 (d, $J = 2.0$ Hz, 2H), 7.46 (q, $J = 4.4$ Hz, 2H), 7.28 (dd, $J = 2.0$, 9.6 Hz, 2H), 6.96–9.91 (m, 2H), 5.96 (s, 1H); ^{13}C NMR (100 MHz, $\text{DMSO-}d_6$) δ 156.76 (d, $J = 230.9$ Hz), 133.28, 125.89, 125.36 (d, $J = 10.1$ Hz), 120.42, 113.10 (d, $J = 9.7$ Hz), 109.91 (d, $J = 25.9$ Hz), 103.18 (d, $J = 23.7$ Hz), 25.12; HRMS (ESI) calcd for $\text{C}_{18}\text{H}_{11}\text{F}_2\text{N}_3$ [$\text{M} + \text{Na}$] $^+$: 330.0813 found 330.0826; IR ν (cm^{-1}): 3431, 3127, 2924, 2242, 1630, 1583, 1487, 1457, 1346, 1170, 938, 800.

4.2.3. 2,2-Bis(4-chloro-1*H*-indol-3-yl)acetonitrile (**5c**)

Rf = 0.49 (petroleum ether/ethyl acetate = 1: 1); White solid; Yield 79%; m.p.: 230.0 – 235.8°C ; ^1H NMR (400 MHz, $\text{Acetone-}d_6$) δ 10.68

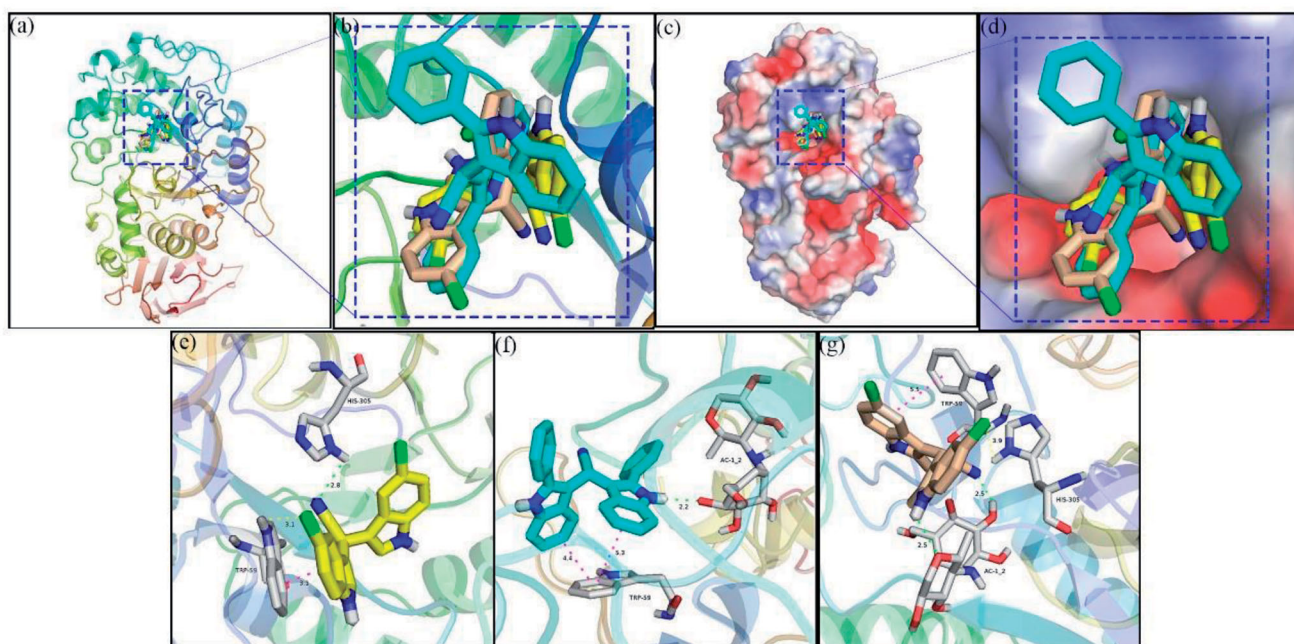


Figure 10. Molecular docking of compounds 5g, 5h, and 5s with α -amylase.

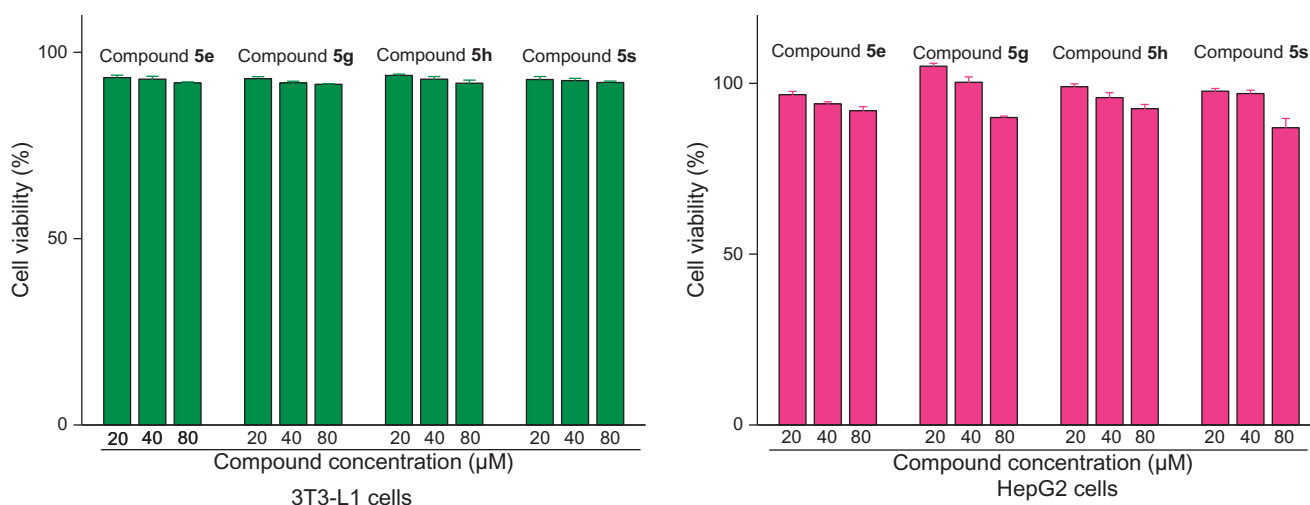


Figure 11. Cytotoxicity assay of compounds 5e, 5g, 5h, and 5s on 3T3-L1 cells and HepG2 cells.

(s, 2H), 7.46 (d, $J=8.0$ Hz, 2H), 7.29 (d, $J=2.8$ Hz, 2H), 7.14 (t, $J=7.6$ Hz, 2H), 7.08 (d, $J=7.2$ Hz), 6.87 (s, 1H); ^{13}C NMR (100 MHz, Acetone- d_6) δ 139.57, 126.95, 125.95, 123.74, 123.11, 121.71, 121.21, 112.52, 111.95, 27.78; HRMS (ESI) calcd for $\text{C}_{18}\text{H}_{11}\text{Cl}_2\text{N}_3$ $[\text{M}+\text{Na}]^+$: 362.0222, found 362.0235; IR ν (cm^{-1}): 3427, 2925, 2854, 2242, 2192, 1617, 1587, 1486, 1429, 1340, 1186, 938, 777, 764, 737.

4.2.4. 2,2-Bis(5-chloro-1H-indol-3-yl)acetonitrile (5d)

Rf = 0.41 (petroleum ether/ethyl acetate = 1: 1); Yellow solid; Yield 80%; m.p.: 168.0–173.4 $^\circ\text{C}$; ^1H NMR (400 MHz, CDCl_3) δ 8.31 (s, 2H), 7.50 (d, $J=2.0$ Hz, 2H), 7.24 (d, $J=8.4$ Hz, 2H), 7.14–7.10 (m, 4H), 5.48 (s, 1H); ^{13}C NMR (100 MHz, CDCl_3) δ 134.88, 126.18, 125.76, 124.62, 123.10, 119.52, 118.02, 112.77, 109.13, 26.05; HRMS (ESI) calcd for $\text{C}_{18}\text{H}_{11}\text{Cl}_2\text{N}_3$ $[\text{M}+\text{Na}]^+$: 362.0222, found 362.0238; IR ν (cm^{-1}): 3432, 3126, 2244, 1682, 1620, 1572, 1463, 1421, 1340, 1101, 894, 798, 737, 587.

4.2.5. 2,2-Bis(6-chloro-1H-indol-3-yl)acetonitrile (5e)

Rf = 0.59 (petroleum ether/ethyl acetate = 1: 1); White solid; Yield 82%; m.p.: 175.6–178.2 $^\circ\text{C}$; ^1H NMR (400 MHz, $\text{DMSO}-d_6$) δ 11.33 (s, 2H), 7.52 (d, $J=8.8$ Hz, 2H), 7.46 (d, $J=2.0$ Hz, 4H), 7.02 (dd, $J=2.0, 8.4$ Hz, 2H), 6.11 (s, 1H); ^{13}C NMR (100 MHz, $\text{DMSO}-d_6$) δ 136.97, 126.47, 125.01, 123.94, 120.38, 119.83, 119.40, 111.57, 109.55, 25.05; HRMS (ESI) calcd for $\text{C}_{18}\text{H}_{11}\text{Cl}_2\text{N}_3$ $[\text{M}+\text{Na}]^+$: 362.0222, found 362.0236; IR ν (cm^{-1}): 3431, 3127, 2925, 2243, 1621, 1546, 1454, 1402, 1336, 1101, 1062, 907, 804, 737, 592.

4.2.6. 2,2-Bis(7-chloro-1H-indol-3-yl)acetonitrile (5f)

Rf = 0.71 (petroleum ether/ethyl acetate = 1: 1); White solid; Yield 84%; m.p.: 162.2–168.8 $^\circ\text{C}$; ^1H NMR (400 MHz, Acetone- d_6) δ 10.37 (s, 2H), 7.61 (d, $J=8.0$ Hz, 2H), 7.57 (d, $J=2.8$ Hz, 2H), 7.22 (d, $J=7.6$ Hz, 2H), 7.04 (t, $J=8.0$ Hz, 2H), 6.04 (s, 1H); ^{13}C NMR (100 MHz, Acetone- d_6) δ 134.84, 128.23, 125.75, 122.44, 121.28, 120.50, 118.61, 117.54, 112.10, 26.70; HRMS (ESI) calcd for

$C_{18}H_{11}Cl_2N_3$ $[M + Na]^+$: 362.0222, found 362.0237; IR ν (cm^{-1}): 3429, 3128, 3069, 2676, 2245, 1622, 1568, 1492, 1436, 1338, 1205, 1194, 1081, 897, 785, 733, 580.

4.2.7. 2,2-Bis(5-bromo-1H-indol-3-yl)acetonitrile (5g)

Rf = 0.42 (petroleum ether/ethyl acetate = 1: 1); White solid; Yield 76%; m.p.: 219.6–223.7 °C; 1H NMR (400 MHz, Acetone- d_6) δ 10.54 (s, 2H), 7.84 (d, J = 0.8 Hz, 2H), 7.54 (d, J = 2.4 Hz, 2H), 7.43 (d, J = 8.8 Hz, 2H), 7.27 (dd, J = 1.6, 8.4 Hz, 2H), 6.00 (s, 1H); ^{13}C NMR (100 MHz, DMSO- d_6) δ 135.27, 126.87, 125.49, 124.18, 120.61, 120.33, 114.05, 111.59, 108.89, 24.79; HRMS (ESI) calcd for $C_{18}H_{11}Br_2N_3$ $[M + H]^+$: 429.9372, found 429.9371; IR ν (cm^{-1}): 3425, 2244, 1709, 1567, 1458, 1419, 1337, 1287, 1263, 1136, 1099, 884, 794, 736, 581.

4.2.8. 2,2-Bis(2-phenyl-1H-indol-3-yl)acetonitrile (5h)

Rf = 0.69 (petroleum ether/ethyl acetate = 1: 1); Yellow solid; Yield 60%; m.p.: 112.0–117.9 °C; 1H NMR (400 MHz, Acetone- d_6) δ 10.67 (s, 2H), 7.93 (d, J = 8.0 Hz, 2H), 7.53–7.50 (m, 6H), 7.35–7.27 (m, 6H), 7.21 (t, J = 7.2 Hz, 2H), 7.07 (t, J = 7.6 Hz, 2H), 6.06 (s, 1H); ^{13}C NMR (100 MHz, Acetone- d_6) δ 137.32, 137.14, 132.74, 129.45, 129.28, 128.96, 128.05, 122.98, 121.46, 120.72, 120.61, 112.40, 107.14, 27.07; HRMS (ESI) calcd for $C_{30}H_{21}N_3$ $[M + Na]^+$: 446.1628, found 446.1640; IR ν (cm^{-1}): 3398, 3058, 2240, 2192, 1890, 1605, 1579, 1488, 1455, 1424, 1340, 1309, 1265, 1246, 1159, 1027, 743, 698, 504.

4.2.9. 2,2-Bis(2-methyl-1H-indol-3-yl)acetonitrile (5i)

Rf = 0.52 (petroleum ether/ethyl acetate = 1: 1); Red solid; Yield 72%; m.p.: 231.2–236.6 °C; 1H NMR (400 MHz, Acetone- d_6) δ 10.17 (s, 2H), 7.63 (d, J = 7.6 Hz, 2H), 7.33 (d, J = 8.0 Hz, 2H), 7.05 (td, J = 0.8, 7.2 Hz, 2H), 6.97 (td, J = 0.8, 7.6 Hz, 2H), 5.95 (s, 1H), 2.45 (s, 6H); ^{13}C NMR (100 MHz, Acetone- d_6) δ 136.29, 133.60, 128.17, 121.75, 121.23, 119.99, 118.92, 111.57, 106.04, 25.13, 12.09; HRMS (ESI) calcd for $C_{20}H_{17}N_3$ $[M + Na]^+$: 322.1315, found 322.1327; IR ν (cm^{-1}): 3396, 3056, 2924, 2238, 2191, 1705, 1620, 1585, 1489, 1460, 1428, 1304, 1263, 1246, 1157, 1017, 743.

4.2.10. 2,2-Bis(4-methyl-1H-indol-3-yl)acetonitrile (5j)

Rf = 0.61 (petroleum ether/ethyl acetate = 1: 1); White solid; Yield 81%; m.p.: 246.2–250.1 °C; 1H NMR (400 MHz, Acetone- d_6) δ 10.32 (s, 2H), 7.31 (d, J = 8.0 Hz, 2H), 7.101–7.095 (m, 2H), 7.05 (t, J = 8 Hz, 2H), 6.46 (d, J = 6.8 Hz, 2H), 6.36 (s, 1H), 2.66 (s, 6H); ^{13}C NMR (100 MHz, Acetone- d_6) δ 138.63, 130.60, 125.37, 125.11, 123.15, 122.55, 122.03, 113.34, 110.74, 30.67, 20.14; HRMS (ESI) calcd for $C_{20}H_{17}N_3$ $[M + H]^+$: 300.1495, found 300.1497; IR ν (cm^{-1}): 3406, 3056, 2926, 2237, 1958, 1752, 1617, 1577, 1459, 1408, 1337, 1263, 1156, 1116, 1048, 764, 742.

4.2.11. 2,2-Bis(5-methyl-1H-indol-3-yl)acetonitrile (5k)

Rf = 0.60 (petroleum ether/ethyl acetate = 1: 1); White solid; Yield 67%; m.p.: 205.1–210.1 °C; 1H NMR (400 MHz, Acetone- d_6) δ 10.20 (s, 2H), 7.45 (s, 2H), 7.33 (d, J = 7.6 Hz, 4H), 6.98 (d, J = 8.4 Hz, 2H), 5.86 (s, 1H), 2.37 (s, 6H); ^{13}C NMR (100 MHz, Acetone- d_6) δ 136.43, 128.99, 126.96, 124.66, 124.47, 121.20, 119.28, 112.40, 110.67, 26.65, 21.71; HRMS (ESI) calcd for $C_{20}H_{17}N_3$ $[M + Na]^+$: 322.1315 found 322.1329; IR ν (cm^{-1}): 3406, 3123, 2922, 2857, 2235, 1626, 1582, 1484, 1422, 1341, 1245, 1096, 1040, 800, 736, 593.

4.2.12. 2,2-Bis(6-methyl-1H-indol-3-yl)acetonitrile (5l)

Rf = 0.75 (petroleum ether/ethyl acetate = 1: 1); White solid; Yield 70%; m.p.: 178.4–183.7 °C; 1H NMR (400 MHz, Acetone- d_6) δ 10.13 (s, 2H), 7.52 (d, J = 8.4 Hz, 2H), 7.31 (d, J = 2.4 Hz, 2H), 7.25 (s, 2H), 6.88 (d, J = 8.4 Hz, 2H), 5.87 (s, 1H), 2.40 (s, 6H); ^{13}C NMR (100 MHz, Acetone- d_6) δ 138.45, 132.30, 124.62, 123.83, 121.89, 121.18, 119.40, 112.46, 111.04, 26.79, 21.79; HRMS (ESI) calcd for $C_{20}H_{17}N_3$ $[M + Na]^+$: 322.1315, found 322.1328; IR ν (cm^{-1}): 3408, 3130, 2921, 2859, 2241, 1711, 1628, 1548, 1454, 1341, 1264, 1246, 1096, 1041, 801, 735, 595.

4.2.13. 2,2-Bis(7-methyl-1H-indol-3-yl)acetonitrile (5m)

Rf = 0.21 (petroleum ether/dichloromethane = 2: 5); White solid; Yield 89%; m.p.: 214.1–219.4 °C; 1H NMR (400 MHz, Acetone- d_6) δ 10.32 (s, 2H), 7.48–7.45 (m, 2H), 7.37 (d, J = 2.8 Hz, 2H), 6.96–6.92 (m, 4H), 5.91 (s, 1H), 2.49 (s, 6H); ^{13}C NMR (100 MHz, Acetone- d_6) δ 137.49, 126.38, 124.19, 123.39, 121.89, 121.11, 120.41, 117.43, 111.70, 26.88, 16.94; HRMS (ESI) calcd for $C_{20}H_{17}N_3$ $[M + H]^+$: 300.1495, found 300.1495; IR ν (cm^{-1}): 3409, 3118, 2922, 2856, 2247, 1835, 1660, 1614, 1437, 1343, 1225, 1122, 1067, 787, 744, 585.

4.2.14. 2,2-Bis(5-fluoro-2-methyl-1H-indol-3-yl)acetonitrile (5n)

Rf = 0.78 (petroleum ether/ethyl acetate = 1: 1); Yellow solid; Yield 80%; m.p.: 183.4–188.0 °C; 1H NMR (400 MHz, Acetone- d_6) δ 10.34 (s, 2H), 7.35 (q, J = 4.4 Hz, 2H), 7.27 (dd, J = 2.8, 10.4 Hz, 2H), 6.87 (dt, J = 2.4, 9.2 Hz, 2H), 5.94 (s, 1H), 2.47 (s, 6H); ^{13}C NMR (100 MHz, Acetone- d_6) δ 158.45 (d, J = 230.7 Hz), 136.12, 132.85, 128.32 (d, J = 10.1 Hz), 120.89, 112.61 (d, J = 9.6 Hz), 109.68 (d, J = 26 Hz), 105.87 (d, J = 4.5 Hz), 103.69 (d, J = 24.4 Hz), 25.09, 12.17; HRMS (ESI) calcd for $C_{20}H_{15}F_2N_3$ $[M + Na]^+$: 358.1126, found 358.1140; IR ν (cm^{-1}): 3410, 2953, 2925, 2855, 2361, 2238, 2191, 1708, 1630, 1583, 1486, 1455, 1265, 1178, 1129, 1089, 847, 798, 601.

4.2.15. 2,2-Bis(2,5-dimethyl-1H-indol-3-yl)acetonitrile (5o)

Rf = 0.22 (petroleum ether/ethyl acetate = 4: 1); White solid; Yield 66%; m.p.: 231.2–236.4 °C; 1H NMR (400 MHz, Acetone- d_6) δ 9.97 (s, 2H), 7.42 (s, 2H), 7.16 (d, J = 8.4 Hz, 2H), 6.85 (dd, J = 1.2, 8.4 Hz, 2H), 5.83 (s, 1H), 2.37 (s, 6H), 2.30 (s, 6H); ^{13}C NMR (100 MHz, Acetone- d_6) δ 134.63, 133.55, 128.65, 128.49, 123.26, 121.31, 118.76, 111.26, 105.62, 25.12, 21.85, 12.15; HRMS (ESI) calcd for $C_{22}H_{21}N_3$ $[M + Na]^+$: 350.1682, found 350.1643; IR ν (cm^{-1}): 3395, 2920, 2236, 1958, 1716, 1587, 1310, 1247, 1028, 869, 735, 591.

4.2.16. 2,2-Bis(5-methoxy-1H-indol-3-yl)acetonitrile (5p)

Rf = 0.69 (petroleum ether/ethyl acetate = (1: 1); Greyish white solid; Yield 84%; m.p.: 118.5–123.0 °C; 1H NMR (400 MHz, DMSO- d_6) δ 10.99 (s, 2H), 7.34 (d, J = 2.4 Hz, 2H), 7.30 (d, J = 8.8 Hz, 2H), 7.05 (d, J = 2.4 Hz, 2H), 6.77 (dd, J = 2.8, 9.2 Hz, 2H), 5.98 (s, 1H), 3.70 (s, 6H); ^{13}C NMR (100 MHz, DMSO- d_6) δ 153.17, 131.61, 125.63, 124.31, 120.71, 112.54, 111.44, 109.10, 100.58, 55.35, 25.06; HRMS (ESI) calcd for $C_{20}H_{17}N_3O_2$ $[M + Na]^+$: 354.1213, found 354.1228; IR ν (cm^{-1}): 3407, 3055, 2937, 2832, 2240, 1715, 1626, 1586, 1487, 1214, 1174, 1027, 925, 802, 737, 623.

4.2.17. Dimethyl 3,3'-(cyanomethylene)bis(1H-indole-5-carboxylate) (5q)

Rf = 0.21 (petroleum ether/ethyl acetate = 4: 1); Red solid; Yield 26%; m.p.: 259.6–266.9 °C; ¹H NMR (400 MHz, DMSO-*d*₆) δ 11.61 (s, 2H), 8.31 (s, 2H), 7.78 (dd, *J* = 1.2, 8.4 Hz, 2H), 7.53–7.48 (m, 4H), 6.37 (s, 1H), 3.82 (s, 6H); ¹³C NMR (100 MHz, DMSO-*d*₆) δ 167.07, 139.27, 125.92, 124.83, 122.71, 121.20, 120.62, 120.50, 112.08, 110.70, 51.80, 24.86; HRMS (ESI) calcd for C₂₂H₁₇N₃O₄ [M + H]⁺: 388.1292, found 388.1292; IR ν (cm⁻¹): 3357, 2959, 2933, 2874, 1723, 1619, 1436, 1285, 1122, 1074, 747.

4.2.18. 2,2-Bis(1-methyl-1H-indol-3-yl)acetonitrile (5r)

Rf = 0.25 (petroleum ether/ethyl acetate = 4: 1); White solid; Yield 84%; m.p.: 70.3–74.6 °C; ¹H NMR (400 MHz, DMSO-*d*₆) δ 7.62 (d, *J* = 7.6 Hz, 2H), 7.42 (t, *J* = 8.4 Hz, 4H), 7.19 (t, *J* = 8.0 Hz, 2H), 7.05 (t, *J* = 8.0 Hz, 2H), 6.10 (s, 1H), 3.75 (s, 6H); ¹³C NMR (100 MHz, DMSO-*d*₆) δ 136.94, 127.90, 125.49, 121.68, 120.65, 119.08, 118.70, 110.08, 108.60, 32.41, 24.93; HRMS (ESI) calcd for C₂₀H₁₇N₃ [M + Na]⁺: 322.1315, found 322.1326; IR ν (cm⁻¹): 3055, 2934, 2239, 1717, 1642, 1615, 1529, 1472, 1374, 1332, 1129, 1013, 742.

4.2.19. 2,2-Bis(5-bromo-1-methyl-1H-indol-3-yl)acetonitrile (5s)

Rf = 0.71 (petroleum ether/ethyl acetate = 1: 1); White solid; Yield 77%; m.p.: 177.7–181.7 °C; ¹H NMR (400 MHz, Acetone-*d*₆) δ 7.78 (s, 2H), 7.40 (t, *J* = 3.6 Hz, 4H), 7.31 (dd, *J* = 2.0, 8.8 Hz, 2H), 5.99 (s, 1H), 3.84 (s, 6H); ¹³C NMR (100 MHz, Acetone-*d*₆) δ 136.48, 128.00, 126.09, 125.53, 121.81, 120.57, 114.49, 113.12, 110.15, 30.67, 26.35; HRMS (ESI) calcd for C₂₀H₁₅Br₂N₃ [M + Na]⁺: 479.9504, found 479.9522; IR ν (cm⁻¹): 3116, 3071, 2923, 2826, 2241, 1725, 1545, 1475, 1376, 1295, 1144, 1047, 856, 793, 737, 706.

4.2.20. 2,2-Bis(1-methyl-1H-pyrrol-3-yl)acetonitrile (6a)

Rf = 0.41 (petroleum ether/ethyl acetate = 4: 1); Brown oily liquid; Yield 56%; ¹H NMR (400 MHz, Acetone-*d*₆) δ 6.72 (t, *J* = 2.4 Hz, 2H), 6.01–5.99 (m, 2H), 5.74 (s, 1H), 3.57 (s, 6H); ¹³C NMR (100 MHz, Acetone-*d*₆) δ 125.11, 124.90, 118.75, 109.76, 107.67, 34.18, 28.67; HRMS (ESI) calcd for C₁₂H₁₃N₃ [M + H]⁺: 200.1182, found 200.1182; IR ν (cm⁻¹): 3105, 2947, 2234, 2177, 1597, 1492, 1305, 1092, 772, 755, 720, 607.

4.2.21. 2,2-Bis(5-methyl-1H-pyrrol-3-yl)acetonitrile (6b)

Rf = 0.25 (petroleum ether/ethyl acetate = 4: 1); Brown oily liquid; Yield 58%; ¹H NMR (400 MHz, Acetone-*d*₆) δ 9.77 (s, 2H), 5.94 (s, 2H), 5.69 (s, 2H), 5.39 (s, 1H), 2.17 (s, 6H); ¹³C NMR (100 MHz, Acetone-*d*₆) δ 129.50, 124.00, 119.56, 108.10, 106.63, 12.16; HRMS (ESI) calcd for C₁₂H₁₃N₃ [M + H]⁺: 200.1182, found 200.1182; IR ν (cm⁻¹): 3336, 2924, 2854, 2196, 1958, 1688, 1588, 1489, 1399, 1042, 776.

4.2.22. 2,2-Di(1H-pyrrol-3-yl)acetonitrile (6c)

Rf = 0.21 (petroleum ether/ethyl acetate = 4: 1); Brown oily liquid; Yield 62%; ¹H NMR (400 MHz, Acetone-*d*₆) δ 10.13 (s, 2H), 6.78 (d, *J* = 1.2 Hz, 2H), 6.11 (d, *J* = 1.2 Hz, 2H), 6.05 (d, *J* = 2.8 Hz, 2H), 5.59 (s, 1H); ¹³C NMR (100 MHz, CDCl₃) δ 122.79, 119.44, 117.71, 109.04, 108.32, 29.99; HRMS (ESI) calcd for C₁₀H₉N₃ [M + H]⁺: 172.0869, found 172.0869; IR ν (cm⁻¹): 3364, 2924, 2853, 2196, 1958, 1716, 1586, 1394, 1097, 1040, 730.

4.2.23. Diethyl 2,2'-((cyanomethylene)bis(4,1-phenylene))bis(methylazanediyl)diacetate (7a)

Rf = 0.21 (petroleum ether/ethyl acetate = 4: 1); Light yellow liquid; Yield 83%; ¹H NMR (400 MHz, Acetone-*d*₆) δ 7.22–7.18 (m, 4H), 6.73–6.69 (m, 4H), 5.23 (s, 1H), 4.14–4.09 (m, 8H), 3.04 (s, 6H), 1.20 (t, *J* = 7.2 Hz, 6H); ¹³C NMR (100 MHz, Acetone-*d*₆) δ 171.07, 149.60, 129.06, 126.07, 121.60, 113.15, 61.10, 54.23, 40.85, 39.55, 14.58; HRMS (ESI) calcd for C₂₄H₂₉N₃O₄ [M + H]⁺: 424.2231, found 424.2231; IR ν (cm⁻¹): 2982, 1743, 1601, 1518, 1373, 1290, 1185, 1117, 1028, 946, 835, 770.

4.2.24. Diethyl 2,2'-((cyanomethylene)bis(4,1-phenylene))bis(azanediyl)diacetate (7b)

Rf = 0.61 (petroleum ether/ethyl acetate = 1: 1); White solid; Yield 58%; m.p.: 87.5–93.4 °C; ¹H NMR (400 MHz, CDCl₃) δ 7.11 (d, *J* = 8.4 Hz, 4H), 6.56 (d, *J* = 8.4 Hz, 4H), 4.94 (s, 1H), 4.37 (s, 2H), 4.24 (q, *J* = 6.8 Hz, 4H), 3.87 (s, 4H), 1.29 (t, *J* = 8.0 Hz, 6H); ¹³C NMR (100 MHz, CDCl₃) δ 170.82, 146.65, 128.62, 125.71, 120.50, 113.16, 61.36, 45.62, 40.94, 14.13; HRMS (ESI) calcd for C₂₂H₂₅N₃O₄ [M + H]⁺: 396.1918, found 396.1918; IR ν (cm⁻¹): 3398, 2983, 2936, 2241, 1739, 1614, 1522, 1374, 1211, 1024, 823.

4.2.25. Dimethyl 2,2'-((cyanomethylene)bis(4,1-phenylene))bis(azanediyl)diacetate (7c)

Rf = 0.39 (petroleum ether/ethyl acetate = 4: 1); White solid; Yield 61%; m.p.: 135.7–140.8 °C; ¹H NMR (400 MHz, CDCl₃) δ 7.12 (d, *J* = 8.4 Hz, 4H), 6.56 (d, *J* = 8.4 Hz, 4H), 4.94 (s, 1H), 4.16 (s, 2H), 3.89 (s, 4H), 3.77 (s, 6H); ¹³C NMR (100 MHz, CDCl₃) δ 171.35, 146.59, 128.64, 125.83, 120.45, 113.21, 52.23, 45.46, 40.94; HRMS (ESI) calcd for C₂₀H₂₁N₃O₄ [M + H]⁺: 368.1605, found 368.1605; IR ν (cm⁻¹): 3390, 2900, 2239, 1727, 1614, 1520, 1436, 1361, 1215, 1179, 991, 810.

4.3. α-Glucosidase inhibition activities and mechanism assay

The α-glucosidase inhibitory activity of compounds **5a–c**, **6a–c**, and **7a–c** were performed according to our previous report.^{30,31} The 10 μL of α-glucosidase enzyme (final concentration 0.1 U/mL) and 10 μL of test compounds (dissolved in DMSO) were added into 130 μL of phosphate buffer (0.1 M, pH 6.8), followed 10 min incubation at 37 °C. Then 50 μL of PNPG (final concentration 0.25 mM) was added, and mixture was continually incubated for 20 min at 37 °C. The absorbance at 405 nm was measured using Multimodel Reader. The percentage of enzyme inhibition was calculated: % Inhibition = [(A₁ - A₀)/A₀] × 100%, where A₁ was the absorbance with the test compound, and A₀ was the absorbance without the test compound. The IC₅₀ value of compound was obtained from the plot of inhibition percentage vs test compound at different concentrations. Acarbose was used as the positive control. The experiment was performed in duplicate.

The inhibition mechanism of compounds **5g**, **5e**, and **5h** was analysed using similar above method. The enzyme inhibitory kinetics was detected using plots of enzyme concentration vs remaining enzyme activity at different inhibitor concentrations, and the substrate inhibitory kinetics was obtained from Lineweaver-Burk plot of remaining enzyme activity vs substrate concentration in the presence of different inhibitor concentrations.³²

4.4. α -Amylase inhibition activities and mechanism assay

The α -amylase inhibitory activity of all tested compounds was performed according to previous report.^{33,34} A 10 μ L of α -amylase enzyme solution (final concentration 0.25 U/mL), 10 μ L of test compounds (dissolved in DMSO), and 80 μ L of phosphate buffer (20 mM, pH 6.9) were mixed and incubated for 10 min at 37 °C. Next, 100 μ L starch solution (final concentration 0.5%) was added into the mixture followed by an incubation of 10 min. After 100 μ L DNS (containing 1 M Potassium sodium tartrate and 48 mM 3,5-Dinitrosalicylic acid) was added, the mixture was kept incubated in boiling water for 15 min. Finally, the absorbance was measured at 540 nm after dilution of solution by adding 900 μ L distilled water. The percentage of enzyme inhibition was calculated: % Inhibition = $[(A_1 - A_0)/A_0] \times 100\%$, where A_1 was the absorbance with the test compound, and A_0 was the absorbance without the test compound. The IC_{50} value of compound was obtained from the plot of inhibition percentage vs test compound at different concentrations. Acarbose was used as the positive control. The experiment was performed in duplicate.

The inhibition mechanism of compounds **5g**, **5h**, and **5S** was also analysed. The enzyme inhibitory kinetics was detected using plots of enzyme concentration vs remaining enzyme activity at different inhibitor concentrations, and the substrate inhibitory kinetics was obtained from Lineweaver-Burk plot of remaining enzyme activity vs substrate concentration in the presence of different inhibitor concentrations.

4.5. Molecular docking

Molecular docking was conducted to explore the interaction of inhibitors with α -glucosidase and α -amylase using Sybyl (Version 2.1.1, Tripos, US) according to our previous report.³³ The crystal structure of α -glucosidase (PDB: 3AJ7)^{33,35} and α -amylase (PDB: 3BAJ)^{36,37} were obtained from the Protein Data Bank. Compounds were prepared with addition of hydrogen atoms, addition of charge with Gasteiger-Hückle mode, and energy minimisation. Then the protein was prepared by procedure of removing H₂O, fixing side chain amides, and adding hydrogens. The active site of α -glucosidase was simulated out using automatic mode. The active site of α -amylase was simulated out using Ligen mode. Then, the docking simulations between compounds and α -glucosidase or α -amylase were carried out with the default format of Pymol program.

4.6. Cell cytotoxicity assay

The 3T3-L1 cells or HepG2 cells were cultured in DMEM medium containing 10% foetal bovine serum, 100 U/mL penicillin and 0.1 mg/mL streptomycin in a humidified incubator with a 5% CO₂ atmosphere at 37 °C. Cells in the logarithmic growth phase were used for this assay. After 5×10^3 3T3-L1 cells were seeded in 96 well plates for 24 h, compound with different concentration was added into each well for 24 h. MTT reagent (100 μ L, 0.5 mg/mL) was added to each well for 4 h incubation. After the supernatant was discarded, 100 μ L of DMSO was added. The absorbance was measured at 490 nm. Each sample was performed in 3 parallel experiments.

Disclosure statement

No potential conflict of interest was reported by the author(s).

Funding

This work was supported by the NSFC [21472077 and 21772071], the Department of Education of Guangdong Province [2017KSYS010, 2019KZDXM035].

References

1. Wang JW, Lv X, Xu JW, et al. Design, synthesis and biological evaluation of vincamine derivatives as potential pancreatic β -cells protective agents for the treatment of type 2 diabetes mellitus. *Eur J Med Chem* 2020;188:111976
2. Tahrani AA, Bailey CJ, Del Prato S, Barnett AH. Management of type 2 diabetes: new and future developments in treatment. *Lancet* 2011;378:182–97.
3. Rafique R, Khan KM Arshia, et al. Synthesis of new indazole based dual inhibitors of α -glucosidase and α -amylase enzymes, their *in vitro*, *in silico* and kinetics studies. *Bioorg. Chem* 2020;94:103195.
4. Dhameja M, Gupta P. Synthetic heterocyclic candidates as promising α -glucosidase inhibitors: an overview. *Eur J Med Chem* 2019;176:343–77.
5. Guerreiro LR, Carreiro EP, Fernandes L, et al. Five-membered iminocyclitol α -glucosidase inhibitors: synthetic, biological screening and *in silico* studies. *Bioorg Med Chem* 2013;21:1911–7.
6. Zhong Y, Yu L, He Q, et al. Bifunctional Hybrid enzyme-catalytic metal organic framework reactors for α -glucosidase inhibitor screening. *ACS Appl Mater Interfaces* 2019;11:32769–77.
7. Adib M, Peytam F, Rahmanian-Jazi M, et al. New 6-amino-pyrido[2,3-d]pyrimidine-2,4-diones as novel agents to treat type 2 diabetes: A simple and efficient synthesis, α -glucosidase inhibition, molecular modeling and kinetic study. *Eur J Med Chem* 2018;155:353–63.
8. Salar U, Khan KM, Chigurupati S, et al. New hybrid hydrazinyl thiazole substituted chromones: As potential α -amylase inhibitors and radical (DPPH & ABTS) scavengers. *Sci Rep* 2017;7:16980.
9. Tysoe CR, Caner S, Calvert MB, et al. Synthesis of montbretin A analogues yields potent competitive inhibitors of human pancreatic α -amylase. *Chem Sci* 2019;10:11073–7.
10. Rahim F, Tariq S, Taha M, et al. New triazinoindole bearing thiazole/oxazole analogues: Synthesis, α -amylase inhibitory potential and molecular docking study. *Bioorg Chem* 2019;92:103284
11. Rafique R, Khan KM, Arshia et al. Synthesis, *in vitro* α -amylase inhibitory, and radicals (DPPH & ABTS) scavenging potentials of new N-sulfonohydrazide substituted indazoles. *Bioorg Chem* 2019;94:103410.
12. Miller BR, Nguyen H, Hu CJH, et al. New and emerging drugs and targets for type 2 diabetes: reviewing the evidence. *Am. Health Drug Benef* 2014;7:452.
13. Senthil SL, Chandrasekaran R, Arjun HA, Anantharaman P. *In vitro* and *in silico* inhibition properties of fucoidan against α -amylase and α -D-glucosidase with relevance to type 2 diabetes mellitus. *Carbohydr Polym* 2019;209:350–5.
14. Hameed S, Kanwal F, Seraj R, et al. Synthesis of benzotriazoles derivatives and their dual potential as α -amylase and α -glucosidase inhibitors *in vitro*: Structure-activity relationship, molecular docking, and kinetic studies. *Eur J Med Chem* 2019;183:111677.

15. Channar PA, Saeed A, Larik FA, et al. Design and synthesis of 2,6-di(substituted phenyl)thiazolo[3,2-b]-1,2,4-triazoles as α -glucosidase and α -amylase inhibitors, co-relative Pharmacokinetics and 3D QSAR and risk analysis. *Biomed Pharmacother* 2017;94:499–513.
16. Bell R, Carmeli S, Sar N. Vibrindole A, a metabolite of the marine bacterium, *Vibrio parahaemolyticus*, isolated from the toxic mucus of the boxfish *Ostracion cubicus*. *J Nat Prod* 1994;57:1587–90.
17. Chao WR, Yean D, Amin K, et al. Computer-aided rational drug design: A novel agent (SR13668) designed to mimic the unique anticancer mechanisms of dietary indole-3-carbinol to block Akt signaling. *J Med Chem* 2007;50:3412–5.
18. Aggarwal BB, Ichikawa H. Molecular targets and anticancer potential of indole-3-carbinol and its derivatives. *Cell Cycle* 2005;4:1201–15.
19. Sivaprasad G, Perumal PT, Prabavathy VR, Mathivanan N. Synthesis and anti-microbial activity of pyrazolylbisindoles-promising anti-fungal compounds. *Bioorg Med Chem Lett* 2006;16:6302–5.
20. Cho HJ, Seon MR, Lee YM, et al. 3,3'-Diindolylmethane suppresses the inflammatory response to lipopolysaccharide in murine macrophages. *J Nutr* 2008;138:17–23.
21. Jayakumar P, Pugalendi KV, Sankaran M. Attenuation of hyperglycemia-mediated oxidative stress by indole-3-carbinol and its metabolite 3, 3'- diindolylmethane in C57BL/6J mice. *J Physiol Biochem* 2014;70:525–34.
22. Kamal A, Khan MN, Srinivasa Reddy K, et al. An efficient synthesis of bis(indolyl)methanes and evaluation of their anti-microbial activities. *J Enzyme Inhib Med Chem* 2009;24: 559–65.
23. Sashidhara KV, Kumar M, Sonkar R, et al. Indole-based fibrates as potential hypolipidemic and antiobesity agents. *J Med Chem* 2012;55:2769–79.
24. Wang GC, Wang J, Xie ZZ, et al. Discovery of 3,3-di(indolyl)indolin-2-one as a novel scaffold for α -glucosidase inhibitors: *In silico* studies and SAR predictions. *Bioorg Chem* 2017;72:228–33.
25. Taha M, Rahim F, Imran S, et al. Synthesis, α -glucosidase inhibitory activity and *in silico* study of tris-indole hybrid scaffold with oxadiazole ring: As potential leads for the management of type-II diabetes mellitus. *Bioorg Chem* 2017;74:30–40.
26. Fleming FF, Yao L, Ravikumar PC, et al. Nitrile-containing pharmaceuticals: Efficacious roles of the nitrile pharmacophore. *J Med Chem* 2010;53:7902–17.
27. Geng Y, Kumar A, Faidallah HM, et al. C-(α -D-Glucopyranosyl)-phenyldiazomethanes-irreversible inhibitors of α -glucosidase. *Bioorg Med Chem* 2013;21:4793–802.
28. Jabeen F, Shehzadi S, Fatmi MQ, et al. Synthesis, *in vitro* and computational studies of 1,4-disubstituted 1,2,3-triazoles as potential α -glucosidase inhibitors. *Bioorg Med Chem Lett* 2016;26:1029–38.
29. Lei LS, Wang BW, Jin DP, et al. Al(OTf)₃-catalyzed tandem coupling reaction between N,N-disubstituted aminomalonitriles and substituted arenes: a synthesis of 1-cyano-bisindolylmethane analogues. *Adv Synth Catal* 2020;362:2870–5.
30. Xu XT, Deng XY, Chen J, et al. Synthesis and biological evaluation of coumarin derivatives as α -glucosidase inhibitors. *Eur J Med Chem* 2020;189:112013.
31. Taha M, Alshamrani FJ, Rahim F, et al. Synthesis of novel triazinoindole-based thiourea hybrid: A study on alpha-glucosidase inhibitors and their molecular docking. *Molecules* 2019; 24:3819.
32. Taha M, Baharudin MS, Ismail NH, et al. Synthesis, α -amylase inhibitory potential and molecular docking study of indole derivatives. *Bioorg Chem* 2018;80:36–42.
33. Taha M, Shah SA, Imran S, et al. Synthesis and *in vitro* study of benzofuran hydrazone derivatives as novel alpha-amylase inhibitor. *Bioorg Chem* 2017;75:78–85.
34. Salar U, Khan KM, Chigurupati S, et al. New hybrid scaffolds based on Hydrazinyl thiazole substituted coumarin; as novel leads of dual potential; *in vitro* α -amylase inhibitory and antioxidant (dpph and abts radical scavenging) activities. *Med Chem* 2019;15:87–101.
35. Imran S, Taha M, Ismail NH, et al. Synthesis of novel flavone hydrazones: *in-vitro* evaluation of α -glucosidase inhibition, QSAR analysis and docking studies. *Eur J Med Chem* 2015; 105:156–70.
36. Yousuf S, Khan KM, Salar U, et al. 2'-Aryl and 4'-arylidene substituted pyrazolones: As potential α -amylase inhibitors. *Eur J Med Chem* 2018;159:47–58.
37. Yousuf H, Shamim S, Khan KM, et al. Dihydropyridines as potential α -amylase and α -glucosidase inhibitors: synthesis, *in vitro* and *in silico* studies. *Bioorg. Chem* 2020;96:103581.